Original Paper

Computation procedure for the temperature in hot glass Application to the finite element simulation of hollow glass forming

Dominique Lochegnies, Christophe Noiret, Charles Thibaud and Jérôme Oudin

Laboratoire d'Automatique et de Mécanique Industrielles et Humaines, Unité de Recherche Associé au CNRS, Valenciennes (France)

A new incremental procedure is developed for the thermal analysis in 3D glass products considering the one-dimensional analytical solutions for a semi-infinite glass wall. When coupled to a code being capable of computing large mechanical deformations, this allows to analyze efficiently the glass flow during the pressing, self-deformation and blowing processes. The forming of a reference tumbler is analyzed via finite element simulations. For each forming step, the temperature distribution is calculated from the pressing parameters; pertinent results are found for this first application.

Verfahren zur Temperaturberechnung in heißem Glas Anwendung der Finite-Element-Simulation der Hohlglasformgebung

Für die thermische Analyse an dreidimensionalen Glasprodukten wird ein neues inkrementelles Verfahren entwickelt, das die eindimensionalen analytischen Lösungen für eine einseitig begrenzte Glaswand berücksichtigt. Wenn es mit einem Kode verbunden wird, der große mechanische Deformationen berechnen kann, erlaubt dieses Verfahren die erfolgreiche Analyse der Glasströmung während des Preß-, Selbstverformungs- und Blasprozesses. Die Formgebung eines Referenzbechers wird über Finite-Element-Simulationen analysiert. Für jeden Schritt der Formgebung wird die Temperaturverteilung an Hand der Preßparameter berechnet; für eine erste Anwendung geeignete Ergebnisse werden erzielt.

1. Introduction

Pressing, self-deformation and blowing are the three principal forming processes to produce axisymmetric hollow glass items (such as bottles, tumblers, vases, cups, ashtrays, test tubes or baby's feeding bottles). For many products (tumblers for example), these three processes are successively linked to obtain the glass item desired. During the step of pressing, the tumbler is only preformed: the glass drop is placed in the first mould, and a plunger presses it to form a parison with a height of up to 70 % of the final tumbler height. For the next step, the parison is introduced to the second mould corresponding to the final tumbler form. During the following second forming due to the action of self-deformation, the parison becomes longer until it nearly reaches the base of the mould. Then, at the step of blowing, pressure is applied to the interior, which is stopped when the tumbler is entirely shaped (i.e. when it has the same shape as the mould). With such a method of manufacturing, the item quality depends greatly on the geometrical constraints, especially on the glass thickness distribution of the final product. The achievement of this final item quality and the competition of the packaging manufacturers compel the glass industry today more and more to master and optimize its production methods. Thus, the supply of the numerical tools is essential.

Received June 6, 1995, revised manuscript March 28, 1996.

Many papers concerning glass item production refer to experimental investigations of the mechanical and thermal properties of glass. The main result with regard to the mechanical properties is the determination of the incompressible linear viscoplastic behaviour (Newtonian type [1]) with a temperature-dependent viscosity [2]. It is now a fact that the control of the strain rate evolution during the forming processes is important. With the strain exceeding a critical limit, the glass flow becomes non-linear and can drastically affect the workability [3]. Concerning the thermal properties of glass, the evolution of the heat transfer phenomena at the glass/mould interface [4] and the contact thermal resistance during the forming processes [5] have been particularly examined.

As for the analysis of the glass item manufacture, most experimental and numerical studies of the pressing step are only interested in the investigation of the thermal contact between glass and mould during pressing [6] and the thickness influence on the temperature distribution in the glass [7]. The finite element simulation of the pressing step is rarely treated. To their knowledge, for the first time, the present authors have proposed a finite element solution with adiabatic boundary conditions [8]. Self-deformation and blowing have been studied more often with the finite element solution methods being different with respect to coupled thermomechanical formulation [9 and 10]. Unfortunately, with this coupling, the model takes a lot of CPU (Central

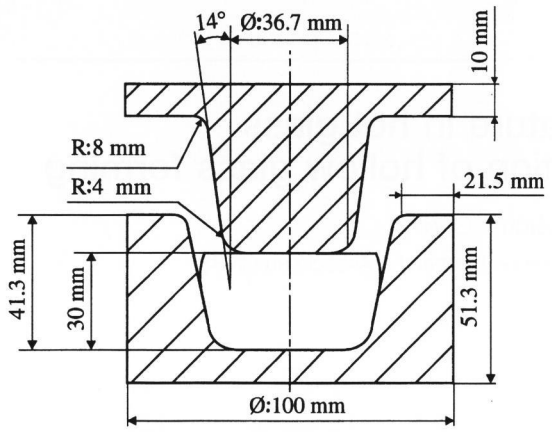

Figure 1. Dimensioning of the glass drop, the plunger and the mould for the first pressing step of the glass tumbler forming process.

Table 1. Significant viscosity values and equivalent strain rates of the NBS-710 standard glass

temperature in °C	viscosity in MPa s^{-1}	critical strain rate for onset of non-Newtonian flow in s^{-1}
500	$3 \cdot 10^{+9}$	$7 \cdot 10^{-8}$
600	$1 \cdot 10^{+4}$	$9 \cdot 10^{-4}$
700	$1 \cdot 10^{+1}$	$2 \cdot 10^{-1}$
800	$2 \cdot 10^{-1}$	4.
900	$1 \cdot 10^{-2}$	$4 \cdot 10^{+1}$
1000	$1 \cdot 10^{-3}$	$2 \cdot 10^{+2}$
1100	$3 \cdot 10^{-4}$	$6 \cdot 10^{+2}$
1180	$1 \cdot 10^{-4}$	$1 \cdot 10^{+3}$

Processing Unit) time and its implementation in a mechanical finite element framework is tedious. Moreover, the addition of the thermal computation can bring about a problem of mesh compatibility between the two computations which will lead to numerical problems. Consequently, an alternating uncoupled computation approach has been developed [11]. With this, the mechanical problem of forming is incrementally solved. At each increment level, a thermal calculation is carried out on which the evolution of the mechanical properties of the glass for the following increment is based. So, the computer implementation is easier and the finite element computations are also less CPU time-consuming, this effect being continually enforced by the evolution of computer power.

In this finite element framework, the developments concern a new three-field mixed approach to the Newtonian glass flow [12 and 13], using penalty functions for the glass/mould contact condition [14]. It is treated as an iterative Newton-Raphson method using an automatic remeshing procedure [15 and 16]. The authors propose approaching thermal aspects with an uncoupled thermomechanical model. The thermal calculation is carried out at each mechanical increment level. The main idea is to use one-dimensional analytical solutions corresponding to thermal convection or contact glass situations at each point of the surface [17 and 18].

With a CPU time reduction, the pressing step of a reference tumbler is finally analyzed to emphasize the pertinence of the authors' developments.

2. Temperature computation in hot glass under free convection and contact heat transfer

2.1 General glass properties

In the following, the manufacture of a commercial tumbler is considered. In particular the pressing of an NBS-710 standard soda–lime–silica glass (chemical composition (in wt%): 70.5 SiO_2, 8.7 Na_2O, 7.7 K_2O, 11.6 CaO, 1.1 Sb_2O, 0.2 Al_2O_3 and 0.2 SO_3) between an AISI-316 steel mould and an AISI-316 steel plunger is referred to (figure 1).

The stress-strain rate relationship of the molten NBS-710 glass is correctly modelled by the Newtonian viscoplastic law in terms of the equivalent von Mises stress $\bar{\sigma}$ and the equivalent strain rate $\dot{\varepsilon}$ [19 and 20] as follows:

$$\bar{\sigma} = 3\eta(\theta)\dot{\varepsilon}$$

where $\eta(\theta)$ is the viscosity of the glass depending on the temperature θ, the incompressibility of the glass has to be respected by penalty function. It follows (in MPa s) from the VFT (Vogel-Fulcher-Tammann) [2] logarithmic law in the temperature range 500 to 1400 °C:

$$\lg[\eta(\theta)] = A + \frac{B}{\theta - T_0} \tag{1}$$

with A, B, T_0 being characteristic constants of the glass experimentally determined (for the NBS-710 standard glass: $A = 8.655$; $B = 4266$; $T_0 = 264.5\,°C$).

For a given temperature, this model is acceptable as long as the glass strain rate does not exceed the critical strain rate value (table 1). At higher strain rates the glass flow becomes non-Newtonian (i.e. non-linear) [3] and can drastically affect the workability. This critical strain rate value is, however, never exceeded with the speed range of plunger displacement and the glass melt temperature used in this work.

Other mechanical characteristics are:

- the density ($\varrho = 2450\,kg\,m^{-3}$) of the NBS-710 standard glass,
- the acceleration due to gravity ($g = 9.81\,m\,s^{-2}$).

2.2 Free convection and contact heat transfer solution for a semi-infinite glass

The high temperature dependence of the glass viscosity requires control and evaluation of the temperature evolution throughout the whole process. During the

manufacture, the temperature of the glass is influenced by the process time and the thermal boundary conditions:

- free convection with the ambient air; this effect is dominant during self-deformation and blowing,
- heat transfer between the glass and the metal surfaces, especially during pressing and blowing.

Previous papers on pressing [7], self-deformation and blowing [9] have shown that the privileged axis for the thermal exchange in the different operations is perpendicular to the glass surface. Consequently, a solution to the computation of the thermal evolution in the glass can be derived considering one-dimensional analytical solutions [17]; these are obtained by taking a semi-infinite glass wall in equivalent thermal situations into account and are applied to the determination of the temperature along the thickness of the glass product.

So, considering a semi-infinite glass wall with its surface continuously losing heat explained by free convection in the ambient air at θ_{inf} (in °C) (figure 2a), the temperature of a point M inside the glass wall, at a distance x from the surface, at the time τ, is:

$$\theta_M(x,\tau) = \theta_0 + (\theta_{inf} - \theta_0) \cdot \cdot [\mathrm{erfc}(X) - e^{2XY+Y^2}\,\mathrm{erfc}(X+Y)] \quad (2)$$

with $X = \dfrac{x}{2\sqrt{\alpha\tau}}$, $Y = \dfrac{h}{k}\sqrt{\alpha\tau}$, $\alpha = \dfrac{k}{\varrho c}$, $\mathrm{erf}(X) = \dfrac{2}{\sqrt{\pi}}\int_0^X e^{-\eta^2}\,d\eta$,

$\mathrm{erfc}(X) = 1 - \mathrm{erf}(X)$, θ_0 the initial temperature (corresponding to $\tau = 0$), τ the free convection time, h the heat transfer coefficient with the ambient air, ϱ the density, c the specific heat and k the thermal conductivity.

For the NBS-710 standard glass at a uniform initial temperature:

$\theta_0 = 1180\,°C$; $c = 1200\,J\,kg^{-1}\,°C^{-1}$ [1]; $k = 1.8\,W\,m^{-1}\,°C^{-1}$.

For the ambient air:

$h = 20\,W\,m^{-2}\,°C^{-1}$; $\theta_{inf} = 50\,°C$.

As for the heat transfer between the glass and the mould or the plunger, it is due to conduction and radiation exchanges; these are time-dependent [18]. This heat transfer can be correctly modelled by the previous solution now using a time-dependent heat transfer coefficient [18].

Considering the semi-infinite glass wall with its surface now in contact with the mould or the plunger, the temperature of which is θ_{inf} (in °C) for the time t (figure 2b), the analytical solution for a point inside the glass wall at a distance x from the interface is obtained from equation (2) by substituting the convection time τ for the contact time t; thus, only X and Y have to be modified by:

[1] Because all temperatures in this paper are expressed in °C, the authors always use this unit, but remember: $1\,J\,kg^{-1}\,°C^{-1} \triangleq 1\,J\,kg^{-1}\,K^{-1}$.

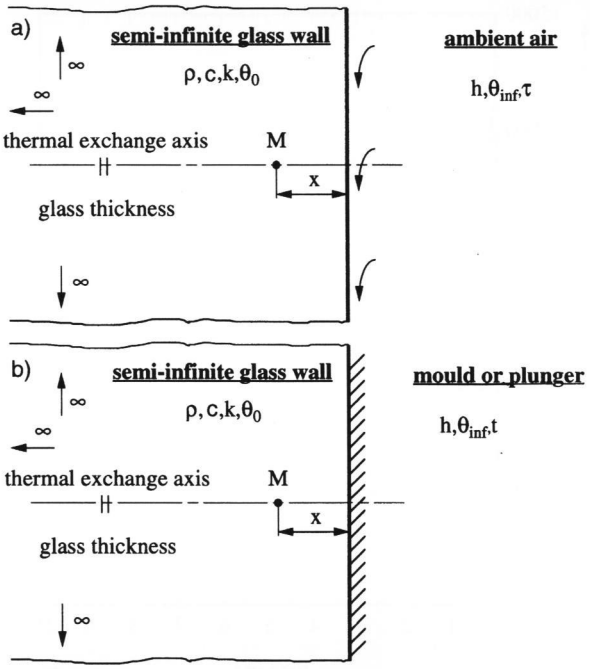

Figures 2a and b. Semi-infinite glass wall (density ϱ (in $kg\,m^{-3}$); specific heat c (in $J\,kg^{-1}\,°C^{-1}$); conductivity k (in $W\,m^{-1}\,°C^{-1}$)) at θ_0 (in °C) initial temperature, a) exposed to the ambient air (heat transfer coefficient h (in $W\,m^{-2}\,°C^{-1}$)) at θ_{inf}(in °C) temperature during the free convection time τ (in s); b) in contact with a mould or a plunger (heat transfer coefficient h (in $W\,m^{-2}\,°C^{-1}$)) at θ_{inf} (in °C) temperature during the heat transfer time t (in s).

$$X = \frac{x}{2\sqrt{\alpha t}} \quad \text{and} \quad Y = \frac{h(t)}{k}\sqrt{\alpha t}\,.$$

For the contact between the NBS-710 standard glass at a uniform initial temperature θ_0 = 1180 °C and the AISI-316 steel mould and plunger at a uniform initial temperature θ_{inf} = 480 °C, the time-dependent function h is given in figure 3.

2.3 Application to a thin glass product

In the hollow glass manufacture, the wall of the product is generally thin (a few millimetres) and the boundary conditions are always represented by free convection and heat transfer through the glass/mould or the glass/plunger contact surface. This heat transfer is denoted contact heat transfer. The temperature in a thin glass item, only subjected to free convection and contact heat transfer, is calculated as follows, using the two semi-infinite glass wall formulations.

For a thin glass product (figure 4), the surface S subjected to m boundary conditions (convection and contact), is decomposed into elementary surfaces S_j in such a way that

$$S = \sum_{j=1}^{m} S_j\,.$$

Each surface S_j is exposed to free convection or contact heat transfer denoted as BC_j. Let M be a point inside

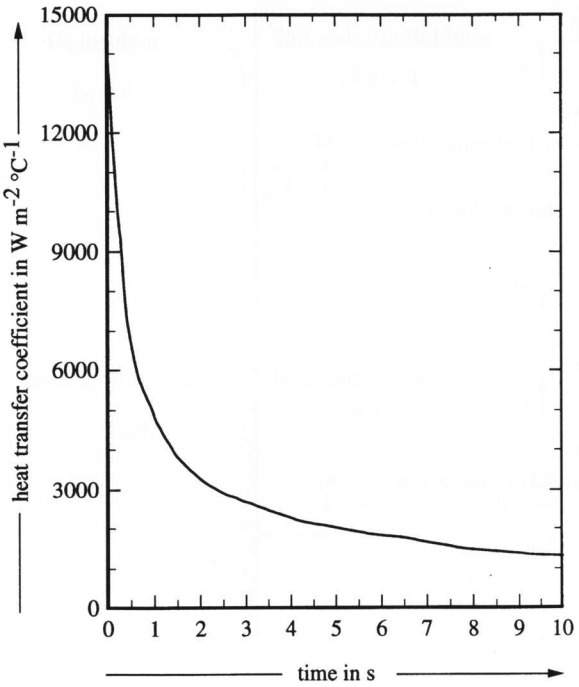

Figure 3. Heat transfer coefficient evolution as a function of time between an NBS-710 standard glass (initial temperature 1180 °C) and an AISI-316 steel mould (initial temperature 480 °C).

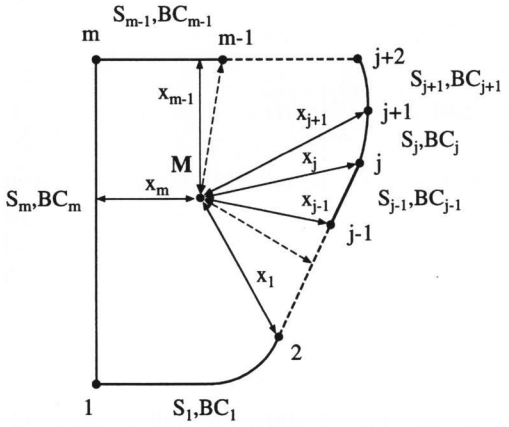

Figure 4. Position of a point M inside the glass volume with regard to the surfaces S_j (with a distance x_j) influenced by the boundary condition BC_j.

the thin glass volume which is located at a distance x_j from each surface S_j, x_j being the minimal distance between M and a point of the surface S_j.

The temperature is then successively adjusted with respect to the elementary surfaces S_j, the distances x_j and the free convection time or the contact time with each boundary using the following expression:

for $j = 1$ to m:

$$\theta_M^j(x, ts) = \theta_M^{j-1} + (\theta_{inf}^j - \theta_0) \cdot \cdot [\mathrm{erfc}(X) - e^{2XY+Y^2}\,\mathrm{erfc}(X + Y)] \quad (3)$$

with $X = \dfrac{x_j}{2\sqrt{\alpha\, ts_j}}$, $Y = \dfrac{h_j}{k}\sqrt{\alpha\, ts_j}$, $\alpha = \dfrac{k}{\varrho C}$, θ_{inf}^j the uniform initial temperature of the boundary condition j, θ_0 the uniform initial temperature of the thin glass, ts_j the contact time t_j or the convection time τ_j, h_j either the heat transfer coefficient of free convection or $h_j = h_j(\tau_j)$ if the heat transfer is via contact.

So, at the end of the computation (3), θ_M^m represents the evaluated temperature at the point M taking all the boundary conditions into account. This temperature evaluation is validated, as follows, with a finite elements simulation.

2.4 Validation for different forming processes of a tumbler

During the forming process of a glass tumbler (figure 5), the glass volume is exposed to heat transfer (with the mould or the plunger) and to free convection (with the ambient air) at each step of the pressing, the self-deformation and the blowing.

To validate the formulation in section 2.3, the temperature evolution as a function of time is computed for each step considering the most critical geometry of the glass volume for the thermal exchange (i.e. the geometry with the minimal thickness); the duration of the thermal exchange is, with this geometry, overestimated throughout the entire duration of the forming step concerned. Indeed, with this geometry the glass is influenced by a more intense heat exchange.

Due to the symmetry of the problem, the thermal computation is only carried out for one half of the glass volume. The boundary conditions at the free surfaces and the surfaces being in contact with the mould and/or the plunger are as described in section 2.3. The symmetry axis is taken as an insulated surface. The properties of the glass, the mould and the plunger, the heat transfer coefficients for the free convection and the direct contact are defined by (see sections 2.1 and 2.2, and figure 3).

The results are compared with a finite element solution using an implicit formulation.

2.4.1 Validation for pressing

The glass geometry corresponds to the final stage of the pressing after 1.5 s (0.5 s pressing and 1 s maintaining contact). The temperature distribution in the glass after 1.5 s is analyzed along five different lines (figure 6) (line 1 crosses the preform at the bottom; line 2 crosses the preform at the lower curvature; line 3 crosses the preform in the area of the slope; line 4 crosses the preform at the higher curvature and line 5 crosses the preform at the top).

The glass volume is influenced by three thermal exchange boundary conditions (BC_1: heat transfer with the mould on the surface S_1; BC_2: free convection with the

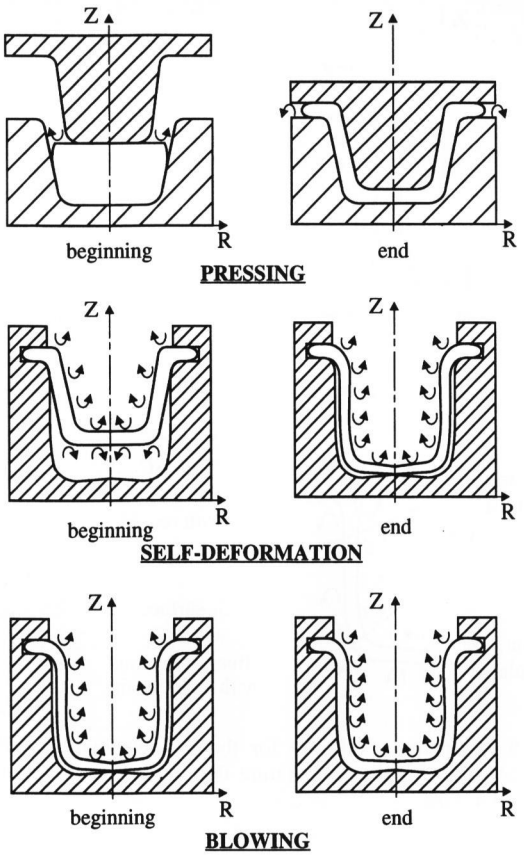

Figure 5. Convection and contact heat exchanges for pressing, self-deformation and blowing steps of the glass tumbler forming process.

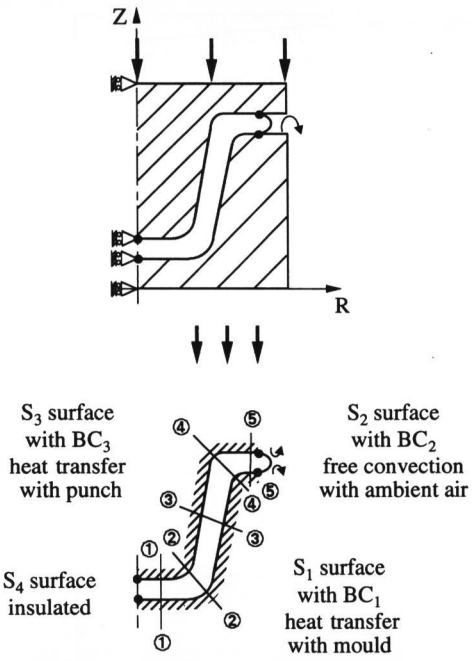

Figure 6. Boundary conditions for the pressing and glass inner lines for the temperature distribution in the glass volume after 1.5 s. Lines 1 to 5 cross the preform at different levels. 1: bottom, 2: lower curvature, 3: area of the slope, 4: higher curvature, 5: top.

ambient air on the surface S_2; BC_3: heat transfer with the mould on the surface S_3; BC_4: insulation at the symmetry surface S_4). The time evolutions of the temperature along the lines 1 to 5 are given in figures 7a to c. Only one half thickness of the glass is regarded due to the symmetry of the boundary conditions for the two computations (equations (3 and 5) are identical to equation (1) due to the same glass thickness).

Inside the glass volume, the error relative to the finite element solution is less than 3.4%. At the glass/mould or the glass/plunger interface, the maximum error relative to the finite element solution is 22% during the first 0.3 s; nevertheless, this error decreases sharply to 5% over 0.3 s; 0.5 s being generally the minimum pressing step duration.

In this simulation, where contact exchanges dominate, a good validation of the developments (error less than 5%) is obtained with a glass thickness close to 5 mm.

2.4.2 Validation for self-deformation

The geometry corresponds to the final stage of the self-deformation; the time, 3.5 s, corresponds to the whole duration of self-deformation. The time evolution of the temperature is compared with the finite element solution along two different lines (figure 8) (line 1 corresponds to the maximum thickness; line 2 corresponds to the minimum thickness).

In this step, the glass volume is influenced by three thermal exchange boundary conditions (BC_1: free convection with the ambient air on the surface S_1; BC_2: heat transfer with the mould on the surface S_2; BC_3: free convection with the ambient air on the surface S_3; BC_4: insulation at the symmetry surface S_4). The temperature evolutions along the lines 1 and 2 are presented in figures 9a and b; again, for the two computations only a half thickness of the glass is considered due to the symmetry of the boundary conditions.

Inside the glass volume and at the glass volume edge, the error relative to the finite element solution is less than 0.5%.

Finally, the developments are also validated for a thermal situation where convection exchanges are the most influential on the temperature distribution in the glass with a thickness close to 4 mm.

2.4.3 Validation for blowing

The glass geometry is the one at the final stage of the blowing; the time is 8 s, corresponding to the blowing time. The temperature evolution with time is analyzed along two different lines (figure 10) (line 1 corresponds to the minimum thickness; line 2 corresponds to the maximum thickness).

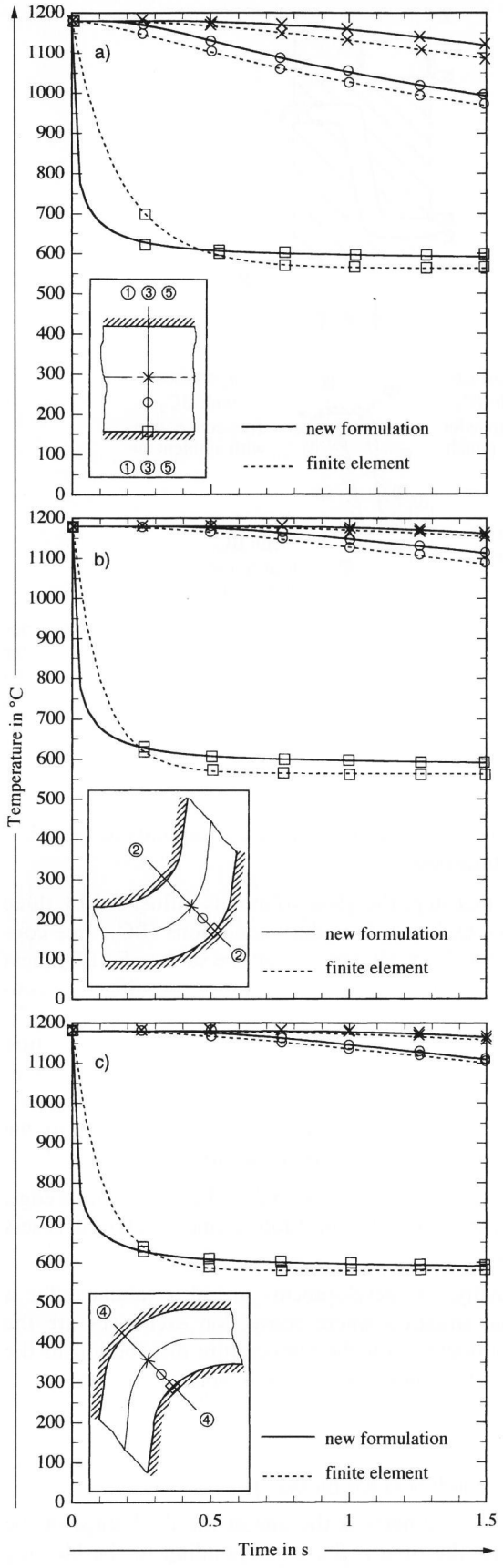

Figures 7a to c. Finite element and 1D temperature distributions in the glass volume along different lines exposed for 1.5 s to heat transfer with the mould and the plunger, a) lines 1, 3, and 5; b) line 2; c) line 4.

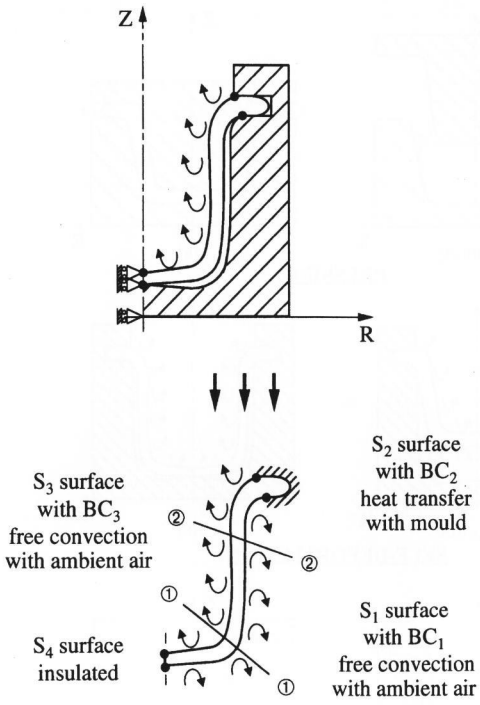

Figure 8. Boundary conditions for the self-deformation and glass inner lines for the temperature distribution in the glass volume after 3.5 s.

The glass volume is now influenced by two thermal exchange boundary conditions (BC_1: heat transfer with the mould on the surface S_1, BC_2: free convection with the ambient air on the surface S_2, BC_3: insulation at the symmetry surface S_3). The temperature evolutions along the lines 1 and 2 are presented in figures 11a and b for the two computations.

The error relative to the finite element solution remains lower than 8% even after 8 s (the blowing duration). The contact with the mould on the whole surface of the glass product is only effective at the end of the blowing after about 3 s.

Even for both contact and convection exchanges, the validation of the developments gives a good correlation (error relative to finite element solution less than 8%), with a glass thickness close to 3.5 mm.

2.5 Conclusions

Using the one-dimensional analytical solutions for a semi-infinite glass wall (exposed to free convection with the ambient air and/or to heat transfer with a metal tool), the authors propose a new solution to evaluate the temperature inside a hollow glass product. The one-dimensional solutions are extended to a three-dimensional body, considering, for a point inside the glass volume, each boundary condition incrementally with the distance between this point and the related boundary surface.

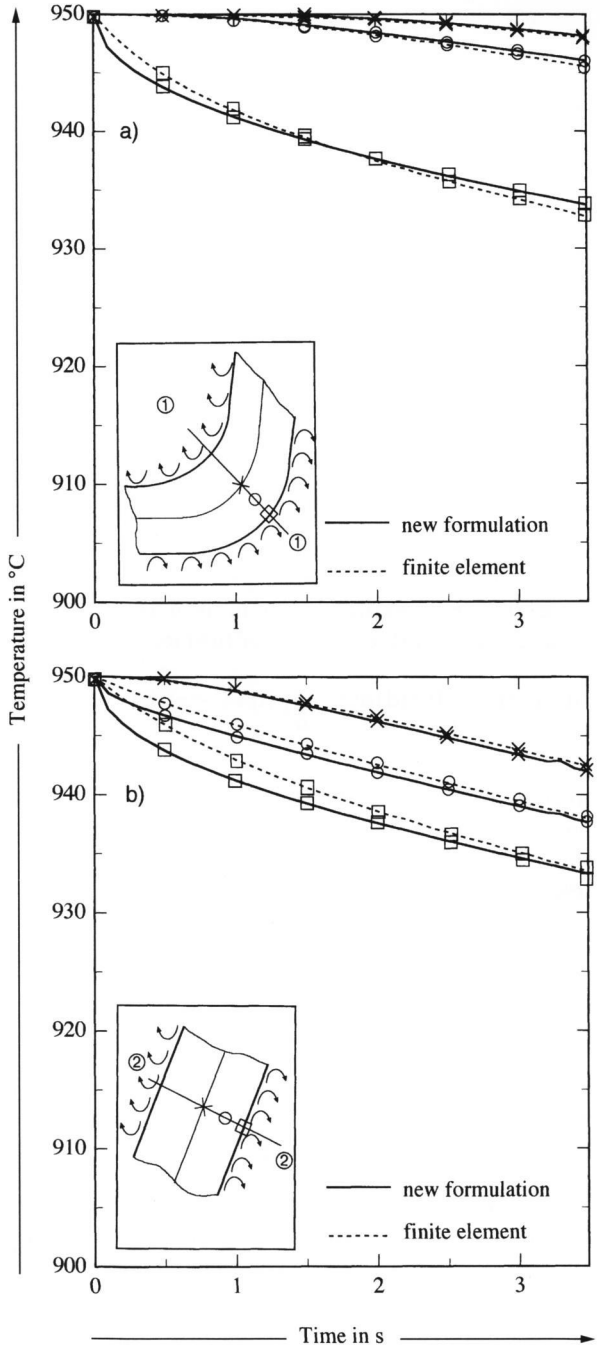

Figures 9a and b. Finite element and 1D temperature distributions in the glass volume along line 1 (figure a) and line 2 (figure b) exposed for 3.5 s to free convection with the ambient air.

With an error less than 8% (in critical reference situations issued from the pressing, the self-deformation and the blowing of a glass tumbler), this solution permits the determination of the varying temperature of a glass product. Its principal interest in comparison with a three-dimensional finite element computation concerns

- the easy computer input,
- the reduced CPU time, and

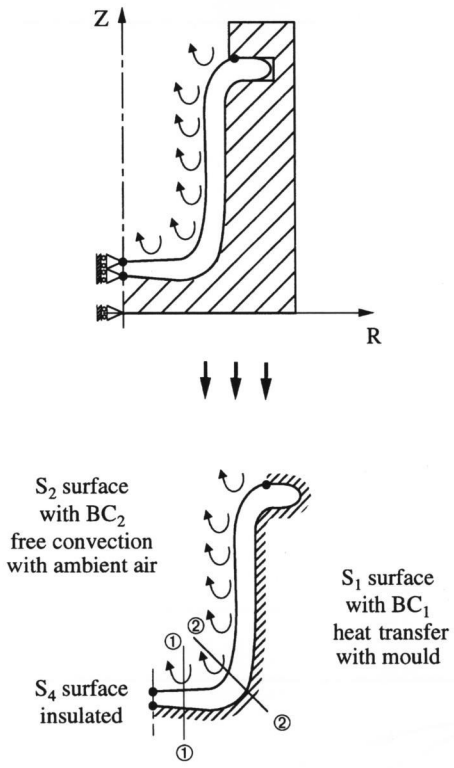

Figure 10. Boundary conditions for the blowing and glass inner lines for the temperature distribution in the glass volume after 8 s.

- the possibility, used in the developments described in section 3., of its implementation in a computer procedure for the analysis of large mechanical deformations of glass products.

3. Uncoupled thermo-viscoplastic formulation

For the glass item forming process, the mechanical problem (related to the large deformation of the parison) and the thermal problem (concerned with the evolution of the glass temperature during forming) are indissociable.

The temperature distribution varies greatly with time, particularly on the product boundaries (i.e. the glass/air, the glass/mould and the glass/plunger interfaces); consequently, this temperature variation involves a viscosity evolution, computed from equation (1).

3.1 Mechanical variation formulation

The bulk behaviour of the glass is correctly modelled by the Newtonian viscoplastic law [1] given by the velocity potential W [8 to 12] as:

$$W(\mathrm{d}) = \frac{3}{2}\eta(\theta)\,\|\mathrm{d}\|^2 \tag{4}$$

where d is the deviatory part of the strain rate tensor D ($\mathrm{d} = D - \{(D_{11} + D_{22} + D_{33})/3\}I$, I the second-order

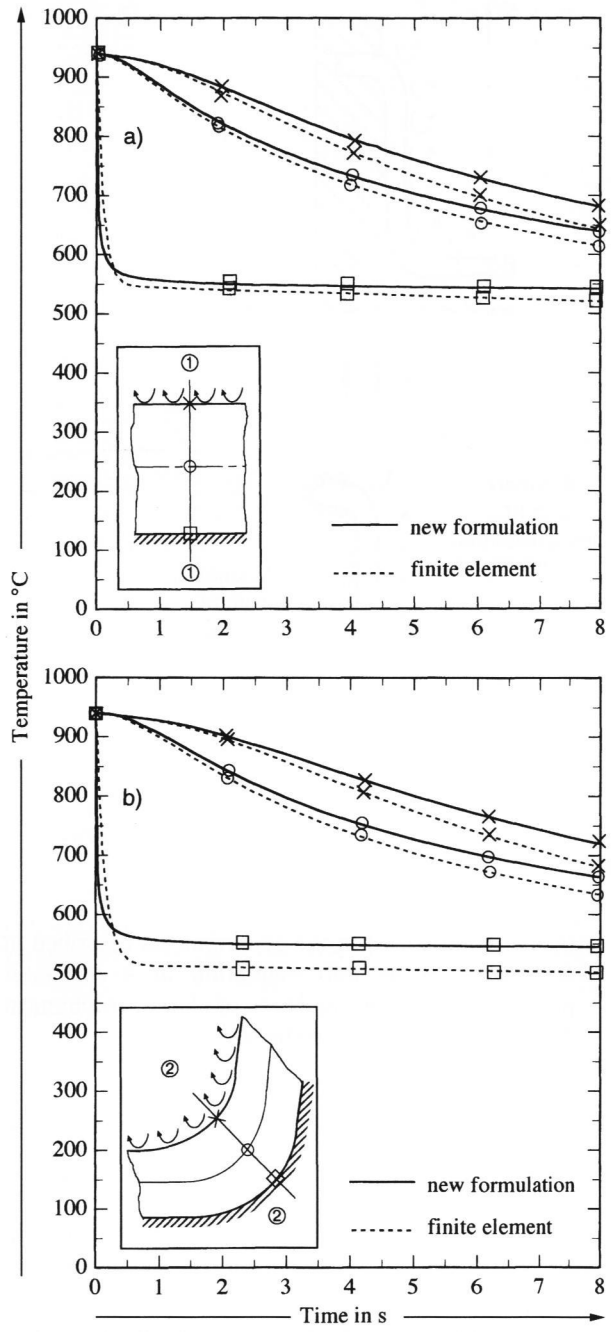

Figures 11a and b. Finite element and 1D temperature distributions in the glass volume along line 1 (figure a) and line 2 (figure b) exposed for 8 s to free convection with the ambient air and to heat transfer with the mould.

unit tensor), $\eta(\theta)$ the viscosity of the glass at the temperature θ. $\|\mathrm{d}\|$ represents the d tensor norm expressed by

$$\|\mathrm{d}\| = \{\mathrm{d}_{11}^2 + \mathrm{d}_{22}^2 + \mathrm{d}_{33}^2 + 2D_{12}^2 + 2D_{13}^2 + 2D_{23}^2\}^{1/2}.$$

The derivative of W with respect to D leads to the deviatory part of the Cauchy stress tensors σ:

$$\sigma = \frac{\partial W}{\partial D} = 3\eta(\theta)\,\mathrm{d}\,.$$

The velocity potential W (equation (4)) only gives the deviatory part of σ; to obtain the mean stress in the glass volume, the following modified potential W^* is usually introduced:

$$W^*(D) = W(\mathrm{d}) + \frac{K}{2}e^2$$

with K a penalty factor, $e = \mathrm{tr}D$ and thus, $D = \mathrm{d} + \frac{\mathrm{tr}D}{3}I$; the incompressibility of the glass ($e = 0$) is successfully achieved taking K values greater than $10^6\,\eta(\theta)$.

With this penalty method, the velocity solution to the incompressible Newtonian flow is established and then the glass pressure field is obtained.

In order to obtain a direct pressure estimation and more suitable stress distribution in the glass, the authors have developed a three-parameter field formulation [12]:

$$G(\upsilon, e, p) = \int_{\Omega} W^*(\mathrm{d})\,\mathrm{d}\Omega - \int_{\Omega} p(\mathrm{tr}\nabla\upsilon - e)\,\mathrm{d}\Omega - \int_{\Gamma_t} t\upsilon\,\mathrm{d}\Gamma_t \qquad (5)$$

where Ω is the glass volume, its surface Γ being decomposed in Γ_υ and Γ_t. Γ_υ, where the velocities υ are prescribed and Γ_t, where the surface tractions t are prescribed. ∇ represents the nabla operator, tr the trace of the tensor ∇_υ.

3.2 Solution for the glass/mould and glass/plunger contacts

During the three-step forming, the contact conditions between the glass and the tools change with time (figure 5). So, the authors have proposed defining the mould or the plunger boundaries by a set of equations $\psi(x, t) = 0$, at time t (with the concention $\psi(x, t) < 0$ if the x coordinate node is located inside the mould or the plunger, $\psi(x, t) > 0$ if the x coordinate node is located outside, $\psi(x, t) = 0$ if the x coordinate node is located on the mould or the plunger boundary) [13].

The contact is examined incrementally; after each Δt time increment, the glass node position has to fulfill:

$$\Psi(x + \upsilon\Delta t, t + \Delta t) \geq 0 \qquad (6)$$

where $\upsilon\Delta t$ is the displacement of the x coordinate node during the time Δt.

The solution to keep to the contact constraints (equation (6)) for the deformed glass body Ω is an external penalization of the potential energy function (5) as:

$$G^*(\upsilon, e, p) = G(\upsilon, e, p) + \frac{\alpha}{2}\{\psi(x + \upsilon\Delta t, t + \Delta t\}^2 \qquad (7)$$

where α is a large positive number. With a basic set of 2D and 3D primitive boundary surfaces for the descrip-

tion of a classical contactor, the authors have developed efficient algorithms for contact interiority and sliding and an automatic procedure to keep to the contact [14].

3.3 Uncoupled thermomechanical solution

In the finite element framework, the solution to the mechanical problem (i.e., the minimum of the functional $G^*(v, e, p)$ (equation (7)) corresponding to an equilibrium state of the glass body) is found by the Newton-Raphson method because of the contact nonlinearities.

At the $(n+1)$th increment (corresponding to a stage of the pressing step for example), and at the ith iteration of the iterative Newton-Raphson method,

$$D_v^2 G^*(v_{n+1}^{(i)}, \eta)\, \Delta v_{n+1}^{(i+1)} = -D_v G^*(v_{n+1}^{(i)}, \eta) \qquad (8)$$

for all virtual velocity fields η [12]; $D_v^2 G^*(v_{n+1}^{(i)}, \eta)$ is the second linearized η direction derivative of $G^*(v_{n+1}^{(i)}, \eta)$ and $D_v G^*(v_{n+1}^{(i)}, \eta)$ is the linearized η direction derivative of $G^*(v_{n+1}^{(i)}, \eta)$.

The velocity field is then adjusted by $v_{n+1}^{(i+1)} = v_{n+1}^{(i)} + \Delta v_{n+1}^{(i+1)}$ with $v_{n+1}^{(i)} = v_n$ solution at the previous increment n.

To take the thermal evolution into account during mechanical deformation, with the uncoupled thermo-viscoplastic solution the glass temperature will be adjusted, using equation (3) at each mechanical increment level at the end of the iterative solution (8). The contact time τ_j related to each boundary condition BC_j is memorized for each node (if a glass node comes into contact with the mould or the plunger during the mechanical increment, its contact time τ_j is initiated; then, it will increase, according to this node contact but independently of the contact time of each other glass node).

When the temperature evaluation is achieved, the mechanical computation continues with the next increment (corresponding, for example, to a new descent of the plunger) using now for the glass viscosity the new temperature distribution in the product (equation (1)).

3.4 Computation complements and conclusions

For the pressing step, for example, the elements of the initial finite element mesh of the glass drop become very distorted, even after an only partial descent of the plunger, and affect the results. With the evolution of the boundary contact conditions, it is important to generate automatically a new mesh, adapted to a correct mechanical computation. For this purpose, using the boundary of the glass volume, the authors have developed three- and four-node element mesh generation [15 and 16].

Consequently, the temperature and the contact time of each glass node, rather than the mechanical data, are interpolated from the badly adjusted old mesh to the new one.

With the uncoupled thermo-viscoplastic formulation, the 2D numerical simulation of the axisymmetric deformation of a glass drop by pressing, self-deformation and blowing, is now possible; the computation of the temperature, at each mechanical increment level, with the analytical solutions across the glass thickness, notably reduces the CPU time of the thermal computation (compared to a finite element procedure); moreover, it alloys an easy implementation in the framework of computing large mechanical deformations.

4. Application to the pressing step of a reference tumbler

The following finite element models are only concerned with the pressing step during the forming of an axisymmetric tumbler (height: 59 mm, inner diameter: 58 mm, average thickness: 3.5 mm). The main goal of a numerical simulation of this first step is to find out the temperature distribution inside the glass preform; in fact, because of the temperature dependence of the glass viscosity, this will directly control the following self-deformation and blowing operations. Using the uncoupled thermomechanical formulation, the authors propose analyzing numerically the sensitivity of the temperature distribution at the end of the pressing step, according to the plunger displacement speed.

In the industrial field, for the reference tumbler, the pressing duration does not exceed 1.5 s, corresponding to the plunger displacement followed by a tool maintenance stage.

4.1 Computer input

The AISI-316 steel mould and plunger are defined (figure 1) according to the final form of the NBS-710 reference tumbler; taking the axial symmetry into account, they are modelled by twelve geometrical points, twelve linear segments and four arcs of circle (figure 12). The mesh of the initial drop is made up of 158 nodes, 128 Q4 elements and twelve T3 elements for a 56.870 mm^3 glass volume. The initial glass drop and tool temperatures are 1180 and 480 °C, respectively, other thermal and mechanical characteristics being defined in sections 2.1 and 2.2 and figure 3.

For a speed range of the plunger of 50 to 1000 $mm\,s^{-1}$, the finite element simulation of the entire pressing step needs 25 remeshing operations; the final mesh is composed of 394 nodes, 307 Q4 elements and 31 T3 elements for a volume error of 0.78 %.

4.2 Finite element analysis of the glass temperature distribution at the final stage of pressing

The temperature distribution after 1.5 s (corresponding to the plunger displacement time and the maintenance

stage for each plunger speed) is analyzed along five distinct lines (figure 13). Lines 1 and 2 correspond to glass parts with different final thicknesses, but which are in contact with the mould and the plunger from the beginning of the pressing. Lines 3, 4 and 5 correspond to glass parts which successively get in contact during the pressing and which present different final thicknesses.

With the uncoupled thermomechanical finite element formulation, the temperature results (table 2, columns 1, 2 and 4) are given for each line at three positions (at the glass/mould interface, in the glass core and at the glass/plunger interface) for the extreme plunger velocities. At the end of the pressing and maintenance stage (i.e., before the self-deformation), the temperature distribution in the glass preform remains the same for the entire plunger speed range for this tumbler; this is explained by the long duration of the maintenance stage (1 s for the minimum 50 mm s^{-1} plunger speed).

In the glass core, the temperature decreases by 20 to 50 K. and on the glass interfaces its variation is about 600 K; these temperature gradients inside the glass are investigated by the manufacturer for the following self-deformation achievement.

Finally, the authors have proceeded with another numerical simulation, assuming that

- during the pressing, the adiabatic hypothesis (i.e., the glass temperature remains at 1180 °C) is justified (thus, no thermal computation is carried out at the mechanical level increment);
- all the heat transfer occurs during the maintenance stage (i.e., only one thermal computation is carried out of the final pressing geometry, with initial temperatures of 1180 for the glass and 480 °C for the tool; these will then change during the maintenance time). With only twelve remeshings for the simulation of the pressing, the temperature results are summarized in table 2, columns 3 and 5, for the five lines.

The main result ist that, for this tumbler forming, the temperature distribution at the end of the first step is not sensitive to the plunger speed (finite element thermomechanically uncoupled analysis); a correct evaluation of the temperature distribution can be also obtained by this method; the maximum error is only 3% locally in the glass core. In fact, according to section 2.4, the thermal evolution with time is more important at the beginning of contact and remains quasi-constant afterwards. In the present case, the contact evolutions for the two computations are not the same (in the thermomechanically uncoupled solution, the contact zones increase progressively, in the second solution, the contact zones geometry corresponds to the final contact zones geometry); the duration of the maintenance stage finally deletes this difference.

4.3 Conclusions on the pressing step

For the first forming step of the reference tumbler, using the finite element thermomechanical formulation, the temperature distribution can be calculated, which is important for the next forming operations.

For this product, the numerical analysis shows that the heat exchanges have more influence during the maintenance stage (even for the longer pressing durations). In this case, only one thermal computation is necessary and concerns the maintenance stage. Consequently, with a mean 3% error, the CPU time saving is greater than 70%.

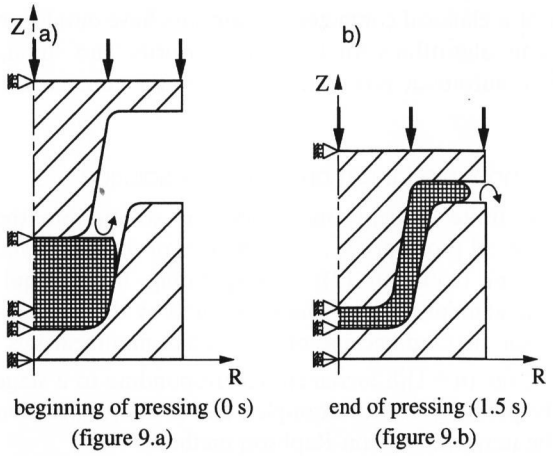

Figures 12a and b. Finite element meshes of the glass drop during pressing; a) initial mesh (initial time 0 s), b) deformed mesh after 1.5 s.

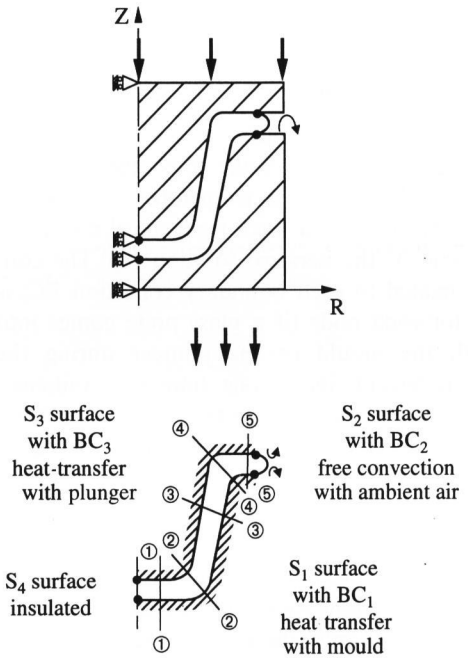

Figure 13. Boundary conditions for the pressing and glass inner lines for the temperature distribution in the glass volume after 1.5 s according to the plunger displacement.

Table 2. Temperature distributions in the glass for the finite element uncoupled thermo-viscoplastic formulations according to different plunger speed values

line no.	position	temperature distribution in °C				
		column 1: 50 mm s^{-1} plunger speed	column 2: 1000 mm s^{-1} plunger speed	column 3: thermal solution	column 4: error in % between columns 1 and 2	column 5: error in % between columns 1 and 3
①	glass/mould	590.85	590.85	590.85	0.00	0.00
	center	1125.20	1122.40	1122.07	0.25	0.28
	glass/plunger	590.85	590.85	590.85	0.00	0.00
②	glass/mould	591.00	591.00	591.00	0.00	0.00
	center	1173.57	1167.12	1166.47	0.55	0.61
	glass/plunger	591.00	591.00	591.00	0.00	0.00
③	glass/mould	593.86	591.05	590.85	0.47	0.51
	center	1150.62	1125.05	1122.07	2.22	2.54
	glass/plunger	591.65	590.97	590.85	0.11	0.14
④	glass/mould	595.56	591.42	591.00	0.70	0.77
	center	1176.88	1169.22	1166.47	0.65	0.89
	glass/plunger	594.39	591.28	591.00	0.52	0.57
⑤	glass/mould	595.86	591.45	590.85	0.74	0.85
	center	1158.11	1126.03	1122.07	2.77	3.21
	glass/plunger	594.54	591.36	590.85	0.53	0.62

5. Conclusions

A new uncoupled thermomechanical formulation has been developed in order to analyze the three forming steps (pressing self-deformation and blowing) of hollow glass item manufacture.

a) The new thermal formulation uses the one-dimensional analytical solutions for a semi-infinite glass wall (exposed to free convection with ambient air and contact with steel tools) for 3D glass products.

b) With less than 8% error (only in critical situations) compared to the finite element solution, this yields a reduced CPU time of computation.

c) In addition, its integration has been achieved, at each increment level, into the viscoplastic three-field formulation, which is based upon an iterative Newton-Raphson method, including contact procedures and remeshing solutions for large deformations.

d) For the pressing of a reference tumbler, the numerical simulations have shown:

- the importance of the maintenance stage on the temperature distribution in the glass before the self-deformation, and
- the efficient numerical analysis of this operation, considering only one final thermal computation after the total adiabatic glass deformation of pressing.

The contact procedures, the related automatic meshing option and the interpolation procedure of the glass state variables are available in the ASTRID finite element code, developed in the Laboratoire d'Automatique et de Mécanique Industrielles et Humaines, Valenciennes (France).

6. References

[1] Simmons, J. H.; Ochoa, R.; Simmons, K. D. et al.: Non-Newtonian viscous flow in soda–lime–silica glass at forming and annealing temperatures. J. Non-Cryst. Solids **105** (1988) p. 313–322.

[2] Fulcher, G. S.: Analysis of recent measurements of the viscosity of glasses. J. Am. Ceram. Soc. **8** (1925) no. 6, p. 339–355.

[3] Simmons, J. H.; Simmons, C. J.: Nonlinear viscous flow in glass forming. Am. Ceram. Soc. Bull. **68** (1989) no. 11, p. 1949–1955.

[4] Huff, N. T.; Shetterly, D. H.; Hibbits, L. C.: Glass to metal heat flow during glass container forming. Glass **57** (1980) no. 12, p. 20/23. (Also in: J. Non-Cryst. Solids **38&39** (1980) p. 873–878.)

[5] Lukisher, E. H. M.; Flow, C. J.: Résistance thermique à l'interface verre/métal et échange thermique lors du formage du verre. (Orig. Russ.) Fiz. Khim. Stekla **10** (1984) no 5, p 630–634.

[6] Fellows, C. J.; Shaw, F.: A laboratory investigation of glass to mould heat transfer during pressing. Glass Technol. **19** (1978) no. 1, p. 4–9.

[7] Kent, R.; Rawson, H.: An experimental and theoretical investigation of glass pressing. Glass Technol. **12** (1971) no. 5, p. 117–127.

[8] Lochegnies, D.; Oudin, J.: Simulations numériques par éléments finis des écoulements newtoniens: Application au formage isotherme du verre. In: 11ème Congrès Français de Mécanique, Lille-Villeneuve d'Ascq (France) 1993. No. 2, p. 29–31.

[9] Rekhson, S.; Zhong-Hao Lu; Day, C. et al.: Computer modelling of glass processing. In: Wilcox, D. L. sr.; Bergeron, C. G. (eds.): 52nd Conference on Glass Problems, Urbana-Champaign, IL (USA) 1991. p. 65–81. (Ceram. Eng. Sci. Proc. **13** (1992) no. 3–4.)

[10] Tateishi, S.; Sasaki, S.; Kobayashi, T.: Coupled thermal-stress analysis of glass blowing process. In: International Conference on Computational Engineering Science, Melbourne (Australia) 1991.

[11] Anderson, H. J.; Liu, G. Q.; Owen, D. R. J.: Computational approaches to the design and forming simulation of glass containers. Klei Glas Keram. **13** (1992) no. 5, p. 150–153.

[12] Lochegnies, D.; Oudin, J.; Picart, P. et al.: Finite element method for large strain viscoplastic problems. In: Owen, D. R. J.; Hinton, E.; Onate, E. (eds.): Proc. Second International Conference on Computational Plasticity, Models, Software and Applications, Barecelona (Spain) 1989. Swansea (UK): Pineridge Press 1989. p. 579–590.

[13] Gelin, J. C.; Lochegnies, D.: Computational methods for constitutive equations with volume constraints in elasto-plastic or elasto-viscoplastic finite deformation. In: Pande, G. N.; Middleton, J. (eds.): Proc. 2nd International Conference on Numerical Methods in Engineering, Theory and Applications, Swansea (UK) 1990. Amsterdam: Elsevier 1990. II, C25.

[14] Lochegnies, D.; Oudin, J.: External penalized mixed functional and related algorithms for unilateral contact and friction in large strain finite element framework. Engineering Computations. (To be publ.)

[15] Matthieu, P.; Oudin, J.; Lochegnies, D. et al.: Automatic mesh refinement procedures in large strain finite element analysis. In: Gruber, R.; Periaux, J.; Shaw, R. P. (eds.): Fifth International Symposium on Numerical Methods in Engineering, Lausanne (Suisse) 1989. Berlin (et al.): Springer 1989. p. 463–468.

[16] Matthieu, P.; Oudin, J.; Lochegnies, D. et al.: Mesh multigeneration, application to two dimensional large strain mechanical problems. In: Pande, G. N.; Middleton, J. (eds.): Proc. 3rd International Conference on Numerical Methods in Engineering, Theory and Applications, Swansea (UK) 1990. Amsterdam: Elsevier 1990. II, C25.

[17] Vriendt, A. B. de: La transmission de chaleur. Morin, G. Editor **1** (1984) p. 257–395.

[18] McGraw, D. A.: Transfer of heat in glass during forming. J. Am. Ceram. Soc. **44** (1961) no. 7, p. 353–363.

[19] Trier, W.: Forming processes of hot glass. In: Mazurin, O. V. (ed.): Glass '89. XVth International Congress on Glass, Leningrad 1989. Survey papers. Leningrad: Nauka 1988. p. 494–515.

[20] Yue, Y.; Brückner, R.: A new description and interpretation of the flow behaviour of glass forming melts. J. Non-Cryst. Solids **180** (1994) p. 66–79.

0896P004

Address of the authors:
D. Lochegnies, C. Noiret, C. Thibaud, J. Oudin
Laboratoire d'Automatique et de Mécanique Industrielles et Humaines
Université de Valenciennes et du Hainaut Cambrésis
BP 311, F-59304 Valenciennes Cédex